Highly repeatable all-solid-state polarization-state generator

X. Steve Yao

Optical Polarization Research Center, Tianjin University, Tianjin, China, and General Photonics Corporation, 5228 Edison Avenue, Chino, California 91710

Lianshan Yan and Yongqiang Shi

General Photonics Corporation, 5228 Edison Avenue, Chino, California 91710

Received December 14, 2004

We report an all solid-state polarization-state generator that uses magneto-optic polarization rotators. The device can generate either five or six distinctive polarization states uniformly across a Poincaré sphere with repeatability better than 0.1°. It is ideal for polarization analysis, swept-wavelength measurement, and monitoring of polarization-related parameters and signal-to-noise ratios of optical networks. © 2005 Optical Society of America

OCIS codes: 120.5410, 080.2730, 060.2300, 260.5430.

Generating at least four distinctive polarization states across a Poincaré sphere with high repeatability, such as at 0°, ±45°, and 90° and right-hand circular (RHC) and left-hand circular (LHC), is important for analyzing polarization properties of light-wave components or systems by use of the Mueller matrix method.[1,2] The information obtained from such analyses can be used to measure other parameters, such as birefringence, polarization mode dispersion, polarization-dependent loss, degree of polarization, signal-to-noise (SNR), and state of polarization (SOP).[3–6] Such a polarization-state generator (PSG) can be constructed from rotating quarter-wave ($\lambda/4$) and half-wave plates.[1] However, owing to its mechanical nature, such a device generally has the disadvantages of slowness, short lifetime, low repeatability, and high cost. A PSG that uses ferroelectric liquid crystals has been reported[4,7]; however, its temperature stability and reliability are concerns for production and field deployment in telecommunication systems. We report what is to our knowledge the first PSG that uses magneto-optic (MO) crystals. For a given wavelength, the device can generate highly repeatable polarization states at 0°, ±45°, and 90° and LHC and RHC across a Poincaré sphere. The measured repeatability is better than 0.1° on the Poincaré sphere. Other advantages of the device are its predictable wavelength and temperature dependence, with typical tolerances of −0.067°/nm and 0.1°/C, respectively. The fiber-to-fiber insertion loss of the device is less than 0.9 dB, and its return loss is better than 55 dB. The same device can also be used as a Mueller matrix polarization analyzer.

As shown in Fig. 1, the five-state PSG consists of an optional polarizer, two pairs (four pieces) of MO rotators, and a $\lambda/4$ plate. The polarizer is placed at the input end of the device, and the $\lambda/4$ plate is sandwiched between the first and the second pairs of MO rotators. The optional polarizer is used for aligning the input SOP with respect to the optical axis (*c* axis) of the $\lambda/4$ plate. The polarizer can be aligned with, orthogonal to, or 45° from the *c* axis of the $\lambda/4$ plate or at other predetermined angles.

Our MO rotator has the following attractive properties: When a positive magnetic field is applied above a saturation field, the rotator rotates the SOP by a precise angle near 22.5°. When a negative magnetic field is applied beyond saturation, the rotator rotates the SOP by a precise angle near −22.5°. Therefore, when both rotators in each pair rotate in the same direction, the net rotation is +45° or −45°. If the two rotators rotate in opposite directions, however, the net SOP rotation is zero. Assuming that the polarizer is aligned with the *c* axis of the $\lambda/4$ plate, the following SOPs can be generated (referenced with respect to the polarizer direction):

(1) A linear SOP at 0° when the rotators in both pairs rotate in opposite directions.
(2) A linear SOP at +45° when the rotators in the first pair rotate in opposite directions but the rotators in the second pair both rotate +22.5°.
(3) A linear SOP at −45°, when the rotators in the first pair rotate in opposite directions but the rotators in the second pair both rotate −22.5°.
(4) RHC, when the rotators in the first pair both rotate 22.5°.
(5) LHC, when the rotators in the first pair both rotate −22.5°.

Note that there are 16 SOP combinations of 4 bits; however, only five states are distinctive and the rest are degenerate. For applications for which only linear

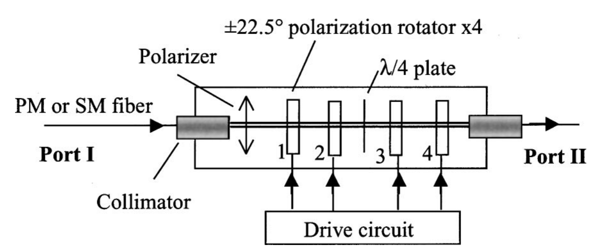

Fig. 1. Schematic of a five-state PSG. For a six-state PSG, two more MO rotators (5 and 6) are added after rotator 4.

Table 1. Six Typical Combinations of MO Switches and Generated Output Polarization States[a]

Rotator						
R1	R2	R3	R4	R5	R6	SOP
+	−	+	−	+	−	0° linear
+	−	+	−	+	+	45°
+	−	+	−	−	−	−45°
+	−	+	+	+	+	90°
+	+	+	+	+	+	RHC
−	−	−	−	−	−	LHC

[a]+ and −, −22.5° and −22.5°, respectively.

SOPs are required, the λ/4 plate can be removed. The device can then generate four linear SOPs, oriented at 0, ±45°, and 90°.

For Mueller matrix calculations, only four distinctive SOPs are required. However, some applications may require six distinctive SOPs for better calibration accuracy. To generate six such polarization states we added another MO rotator pair to the device (after the second pair) to produce additional +45° and −45° rotations. Note that this 6-bit device (with six binary MO switches) can theoretically generate 64 states; however, only six states are nondegenerate. Table 1 lists six typical combinations of this 6-bit device to generate six distinctive SOPs [0° linear, +45° linear, −45° linear, ±90° linear (degenerate), RHC, and LHC]. In the table, R1 stands for rotator 1 and + and − stand for +22.5° and −22.5°, respectively.

We fabricated multiple five- and six-state PSGs and measured their performance with the experimental setup shown in Fig. 2. Using an Agilent 8509C polarization analyzer, we carefully measured the SOPs generated on the Poincaré sphere that corresponded to each activation combination, and the results are shown in Figs. 3(a) and 3(b) for five- and six-state devices, respectively. Points A–E in Fig. 3(a) clearly show five distinctive SOPs generated by the five-state PSG; A is ~LHC, C is ~RHC, D is ~0° linear, B is ~−45° linear, and E is ~45° linear. During the measurement we used the polarization controller in Fig. 2 to align the SOPs with the major axes of the Poincaré sphere. The traces connecting the points show the transient SOP paths when the SOPs are switched from one SOP to another.

Similarly, points A–F in Fig. 3(b) are six distinctive SOPs generated by the six-state PSG. Assuming that a PSG is made with ideal components, many of the bit combinations will produce the same SOP, resulting in so-called degeneracy. However, in practice, because of imperfections of the components used, these supposed degeneracy states are slightly off center and produce a cluster of SOPs in the vicinity of the targeted SOP. This is why we see multiple traces of similar orientation, but with some deviation, passing through each targeted SOP. When we use the device we simply select six bit combinations to generate six consistent SOPs. For example, the bit combinations that correspond to the six SOPs shown in Fig. 3(b) are (010001), (001101), (011101), (011100), (011111), and (111011).

We also measured the wavelength dependence of the devices, and the result is shown in Fig. 4. The vertical axis corresponds to the solid angle between two SOPs separated by ~90° on the Poincaré sphere (~45° of physical rotation). As shown in Fig. 4, a measured solid angle has a linear dependence on wavelength, with a slope of −0.134°/nm. Therefore the physical rotation angle dependence is ~−0.067°/nm. We also found that the wavelength dependence is different for different polarization states.

Note that, for Mueller matrix polarization analysis, the inaccuracies of generated polarization states with respect to the targeted polarization states (0°, +45°, −45°, 90°, RHC, and LHC), such as that caused by wavelength dependence, can be calibrated out in calculations.

SOP repeatability is in fact a more important specification for Mueller matrix analysis because it generally involves taking a reference measurement and device-under-test measurements. The repeatability of the generated SOPs between the reference

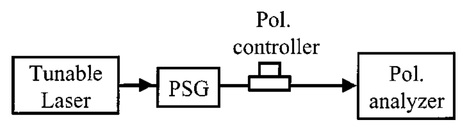

Fig. 2. Measurement setup for characterization of PSGs: Pol., polarization.

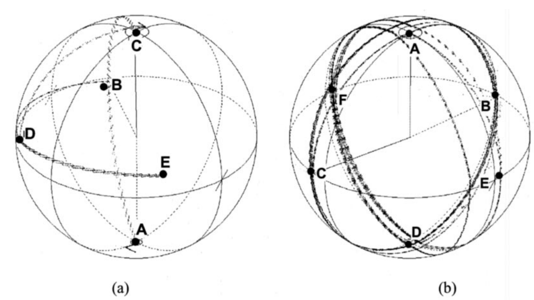

Fig. 3. Poincaré sphere illustration of SOPs generated by the PSG measured with an Agilent 8509C polarization analyzer. SOPs generated by (a) a five-state PSG (b) a six-state PSG.

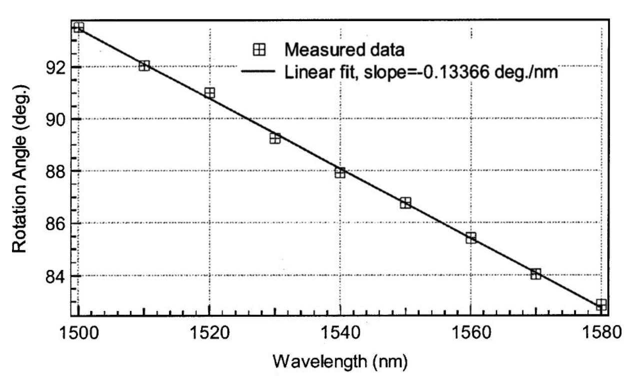

Fig. 4. Wavelength dependence of the polarization rotation angle of the six-state PSG measured on a Poincaré sphere. The physical rotation angle is one-half that measured on the sphere.

measurement and the device-under-test measurements directly affects the accuracy of the resultant Mueller matrix analysis.

Figure 5(a) shows the measured SOP repeatability between polarization states A and B on a Poincaré sphere with 100 samples. As can be seen, the two states (two end points in the figure) are exactly repeatable, with no observable differences. It is interesting to note that the switching traces from A to B and from B to A are highly repeatable as well. However, they are not exactly the same and are interwoven. This trace nonreciprocal property does not affect the performance of the device in any way; however, its cause is still under investigation.

We also evaluated the SOP repeatability of all six states in Fig. 3(b) by repeatedly switching among the states 100 times and measuring the corresponding Stokes parameters of each state. The excellent repeatability of the Stokes parameters of a polarization state is shown in Fig. 5(b). All other five states show the same high repeatability. The solid angles between the states were also calculated for each corresponding sample point, and a typical result is shown in Fig. 5(c), illustrating a high repeatability. The measured solid angle repeatability is better than 0.1°, limited by the accuracy of the measurement system.

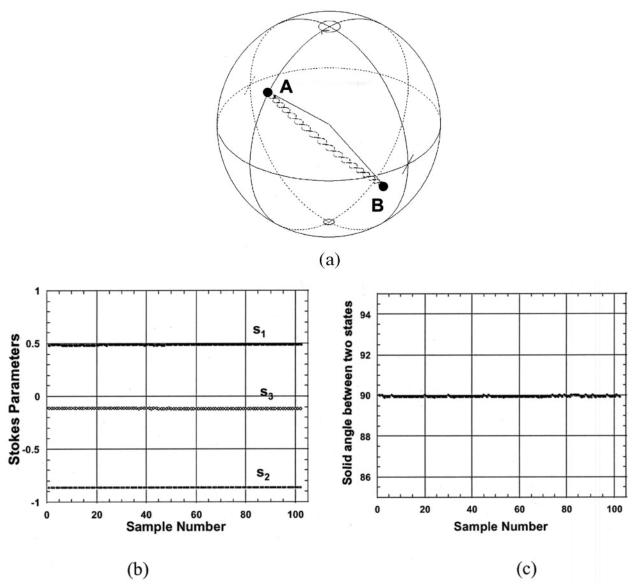

Fig. 5. Repeatability measurement of a six-state PSG [100 samples were taken for each of (a)–(c)]. (a) Poincaré sphere illustration of the repeatability when the device was switched between two polarization states. (b) Stokes parameters illustration of repeatability as a function of sample points. (c) Solid angle illustration of repeatability as a function of sample points. All the measurements show the excellent repeatability of the generated SOPs.

The device may find many applications ranging from polarization analysis to monitoring of network performance, material birefringence, and measurement of polarization mode dispersion, swept-wavelength measurement, medical imaging (e.g., polarization-resolved coherent topology measurement[8–10]), and fiber sensor systems. In particular, the PSG described in Fig. 1 can be used as a polarization analyzer if it is used in reverse order, that is, to input an optical signal from port II into Fig. 1 and detect the signal from port I. Thus two identical devices can be used (i.e., one as a PSG and the other as polarization-state analyzer) to measure or monitor the corresponding properties or perturbation of optical medium. Notably, owing to its high speed and high repeatability, if a spectrum-disperse device, such as a grating or a wavelength-division demultiplexer, is connected to port I, the device can simultaneously analyze multiple wavelength channels in parallel to characterize or monitor various parameters, such as state and degree of polarization as well as polarization mode dispersion and polarization-dependent loss of devices under test.

We thank Lynn Lin for the mechanical design and Jane Chen for assembly of the device. X. S. Yao's e-mail address is syao@generalphotonics.com.

References

1. R. A. Chipman, in *Handbook of Optics*, 2nd ed., M. Bass, ed. (McGraw-Hill, New York, 1995), Vol. II, Chap. 22.
2. D. H. Goldstein and R. A. Chipman, J. Opt. Soc. Am. A **1**, 693 (1990).
3. A. E. Willner, S. M. R. Motaghian Nezam, L.-S. Yan, Z. Pan, and M. C. Hauer, J. Lightwave Technol. **22**, 106 (2004).
4. R. M. Craig, S. L. Gilbert, and P. D. Hale, J. Lightwave Technol. **16**, 1285 (1998).
5. A. Zadok, N. Simon, and A. Eyal, J. Lightwave Technol. **22**, 1533 (2004).
6. M. Petersson, H. Sunnerud, M. Karlsson, and B. E. Olsson, IEEE Photonics Technol. Lett. **16**, 686 (2004).
7. W. Xiang and A. M. Weiner, in *Digest of the LEOS Summer Topical Meetings* (Institute of Electrical and Electronics Engineers, Piscataway, N.J., 2003), p. WB2.4/67.
8. B. H. Park, M. C. Pierce, B. Cense, and J. F. de Boer, Opt. Lett. **29**, 2512 (2004).
9. W. Urbanczyk, Opt. Acta **33**, 53 (1986).
10. A. M. Baldwin, J. R. Chung, J. S. Baba, C. H. Spiegelman, M. S. Amoss, and G. L. Cote, in *Proceedings of the 25th Annual International Conference of the IEEE* (Institute of Electrical and Electronics Engineers, Piscataway, N.J., 2003), Vol. 2, p. 1027.